Adsorption of small aromatic molecules on the (111) surfaces of noble metals: A density functional theory study with semiempirical corrections for dispersion effects

Katrin Tonigold and Axel Groß[a)]
Institute for Theoretical Chemistry, Ulm University, D-89069 Ulm, Germany

(Received 16 March 2010; accepted 10 May 2010; published online 10 June 2010)

The adsorption of benzene, thiophene, and pyridine on the (111) surface of gold and copper have been studied using density functional theory (DFT). Adsorption geometries and energies as well as the nature of bonding have been analyzed and compared to experimental results. Dispersion effects between neighboring molecules and between molecules and the surface have been taken into account via a semiempirical C_6R^{-6} approach. The C_6 coefficients for metal atoms have been deduced using both atomic properties and a hybrid QM:QM approach. Whereas the pure DFT calculations underestimate the adsorption energies significantly, a good agreement with experimental results is obtained using the DFT-D method based on the QM:QM hybrid approach. © *2010 American Institute of Physics*. [doi:10.1063/1.3439691]

I. INTRODUCTION

In recent years, significant progress has been made in the field of organic and molecular electronics based on organic layers deposited on inorganic substrates.[1] For example, optoelectronic devices, built on the basis of π-conjugated molecules, reached the market.[2] In order to further improve or modify their properties, a thorough understanding of the interface between the substrate and the organic layer is crucial.[3] Simple and therefore well-studied aromates such as benzene, thiophene, or pyridine often serve as molecular building blocks for larger molecules used in organic electronics[4] or host-guest networks.[5–7] The adsorption of these molecules on several noble metal surfaces has been studied in detail both experimentally and computationally. Experiments have shown that benzene interacts weakly with (111) surfaces of noble metals.[8–10] It adsorbs in a flat-lying manner and forms ordered (3×3) overlayers.[11] Heteroaromates, such as thiophene or pyridine, were found to undergo a potential or coverage driven phase transition when they are adsorbed on noble metal (111) surfaces from solution[12–17] or under high vacuum conditions:[18–23] in the low coverage regime the heteroaromate adopts a flat-lying conformation, while upon increasing the coverage a tilted or vertical orientation was observed. Among other overlayer structures,[24–26] a (3×3) unit cell for the low coverage phase and a $(\sqrt{3}\times\sqrt{3})R30°$ unit cell for the high coverage phase have been reported.[12,21]

Calculations of such systems based on density functional theory (DFT) reveal significant discrepancies with experiments, in particular concerning adsorption energies.[27–29] The largest portion of these discrepancies is most likely due to the lack of DFT methods to correctly account for dispersion effects. Thus, the application of dispersion corrections in DFT adsorption studies of organic molecules on various substrates has recently gotten in the focus of interest.[30–51] The inclusion of dispersion effects in DFT has been realized by different approaches. For example, it was suggested to adjust effective core potentials in order to model dispersive forces via the atom-electron interactions.[30] A second approach modifies the density functionals themselves in an empirical fashion to get a better description of noncovalent interaction, as done in the work of Truhlar *et al.*[31] A nonlocal functional was proposed by Langreth, Lundqvist, and co-workers.[32] This functional has been successfully applied to the adsorption of molecules on metal surfaces.[33,34] However, this rather expensive method stays restricted to smaller systems.

Furthermore, there is a semiempirical DFT-D approach that adds a C_6R^{-6}-type correction to the Kohn–Sham Hamiltonian. This concept is pursued by many groups[35–43] with different ways to calculate the C_6 coefficients and therefore different degrees of empiricism. The DFT-D approach with C_6 parameters derived from atomic properties has been used for adsorption phenomena such as the adsorption of adenine on graphite.[44] In addition, examples for the application to the adsorption of molecules on metal surfaces exist.[34,45] Three different semiempirical dispersion correction schemes were applied to the adsorption of azobenzene at coinage metal surfaces,[46] yielding the same qualitative, but rather different quantitative results. Recently, C_6 parameters for adsorption phenomena on metal surfaces have also been obtained by first deriving the C_3 coefficient appearing in the z^{-3} interaction between a molecule and a surface and then fitting this to the same interaction expressed as a sum of pairwise van der Waals terms.[48] Another way to derive the parameters of the C_6R^{-6}-type correction is given by a hybrid QM:QM approach.[49–51] In this method, the dispersion energy is approximated as the difference between the adsorption energies according to *ab initio* quantum chemical and DFT calculation for finite portions of the adsorbate-substrate complex.

Considering the variety of different flavors of DFT-D

a)Author to whom correspondence should be addressed. Electronic mail: axel.gross@uni-ulm.de.

 © 2010 American Institute of Physics

Author complimentary copy. Redistribution subject to AIP license or copyright, see http://jcp.aip.org/jcp/copyright.jsp

approaches, in particular as far as the choice of the C_6 parameters are concerned, there is certainly a need to validate the accuracy and transferability of the different methods. In this study, we apply the semiempirical DFT-D approach to the adsorption of small aromates on noble metal surfaces with the C_6 parameters deduced from atomic properties[36,37] as well as from a hybrid QM:QM approach.[49–51] We mainly focus on the adsorption of thiophene on Au(111) because of the outstanding role thiophene and its derivatives play in the field of molecular electronics, but the adsorption of benzene and pyridine on Au(111) and Cu(111) and thiophene on Cu(111) are included in this work in order to derive chemical trends among the small aromatic molecules.

II. METHODS

A. Density functional theory calculations

Periodic DFT calculations have been performed using the Vienna *ab initio* simulation package (VASP).[52,53] Electron-electron exchange and correlation interactions have been described within the generalized gradient approximation (GGA) by employing the Perdew, Burke, and Ernzerhof (PBE) functional.[54] In order to account for electron-ion interactions, the projector augmented wave method[55,56] has been used. The electronic one-particle wave functions were expanded in a plane wave basis setup to an energy cutoff of 400 eV. The metal surfaces were modeled by a slab consisting of five atomic layers that were separated by a vacuum region of 25 Å. The geometry of the adsorption complex was optimized by relaxing all atoms of the adsorbate and the metal atoms of two uppermost layers of the surface. The layer spacing of the lower layers were taken from the theoretical lattice parameters calculated for bulk copper (3.636 Å) and gold (4.171 Å). The adsorption of aromates at a low coverage has been modeled by a (3×3) overlayer structure whereas the adsorption at high coverages has been realized by a $(\sqrt{3}\times\sqrt{3})R30°$ overlayer structure. $4\times4\times1$ and $9\times9\times1$ Monkhorst–Pack k point meshes, respectively, with a Methfessel–Paxton smearing of 0.1 eV were used for the integration over the first Brillouin zone. Isolated molecules in the gas phase were treated employing a large cell (20 Å $\times$21 Å$\times$22 Å), the Γ-point only and a Gaussian smearing of 0.1 eV.

The adsorption energy has been defined as

$$E_{\mathrm{ad}} = E_{\mathrm{tot}} - (E_{\mathrm{surf}} + E_{\mathrm{mol}}), \tag{1}$$

where E_{tot}, E_{surf}, and E_{mol} are the total energy of the relaxed adsorption complex, the energy of the clean surface, and the energy of the isolated molecule, respectively.

B. Corrections for dispersion effects

In order to take dispersion effects into account that are missing in current DFT-functionals we followed the DFT-D approach.[36,37] Thus, the total energy is given by

$$E_{\mathrm{DFT\text{-}D}} = E_{\mathrm{DFT}} + E_{\mathrm{disp}}, \tag{2}$$

where E_{DFT} is the energy obtained from the DFT calculation and E_{disp} is an dispersion correction containing the C_6R^{-6} dependency. We determined E_{disp} as suggested by Grimme[36,37]

$$E_{\mathrm{disp}} = -s_6 \sum_i \sum_j \frac{C_6^{ij}}{R_{ij}^6} f_{\mathrm{damp}}(R_{ij}). \tag{3}$$

The damping function f_{damp}, the scaling factor s_6, and the atomic C_6^{ii} coefficients for nonmetals needed to calculate the dispersion coefficients for mixed atom pairs $C_6^{ij}=\sqrt{C_6^{ii}C_6^{jj}}$ were taken without any further modification from Ref. 37.

Whereas the DFT-D approach is known to yield satisfactory results for molecules containing no metal atoms,[37] there is still a debate going on about the proper DFT-D treatment of metal atoms.[42,43] In order to get the atomic C_6^{ii} coefficients for metals, we have applied two different approaches. In a first approximation, that we will further refer to as the "Grimme method," we calculated the C_6 coefficients for metal atoms in surfaces from atomic properties in the manner Grimme did it for metal-ion containing complexes.[36,37] Being well aware that this simplification might fail, it should serve as a reference for comparison.

The second approach, further called "hybrid method," follows the hybrid QM:QM method that was suggested by Tuma and Sauer[50] and applied to metal surfaces by Hu *et al.*[51] Accordingly, we did both MP2 and DFT-PBE single point energy calculations of the adsorption of aromates on small metal clusters. The dispersion energy was approximated as the difference between the adsorption energy of the MP2 calculation and the adsorption energy of the DFT-PBE calculation. Using this simplification, the C_6 coefficients of the metal atoms could be obtained by a least-squares fitting of the expression to this energy difference. We are well aware that the description of metal clusters using MP2 is problematic because of the large number of electronic states close to the gap between the highest occupied molecular orbital (HOMO) and the lowest unoccupied molecular orbital (LUMO) that cause a slow convergence of the perturbation expansion. Therefore, for smaller clusters with up to six metal atoms we also performed MP3, MP4 and coupled cluster calculations at the CCSD and CCSD(T) level to check the suitability of the MP2 calculations. For larger metal cluster sizes, unfortunately the coupled cluster calculations become prohibitively expensive.

The calculations of the aromate-metal cluster complexes were performed using the GAUSSIAN 03 code.[57] Different effective core potentials for the metal atoms have been used.[58–61] For the atoms of the adsorbate Dunning's correlation consistent basis sets[62,63] or Pople's 6-31G (Refs. 64–68) and 6-311G (Refs. 69 and 70) basis sets were employed. To account for the basis set superposition error the counterpoise method was applied.[71]

The term "adsorption energy" might be misleading in conjunction with interactions between aromates and very small clusters. In the course of this article, this energy is also simply called "interaction energy" and has been defined in an analogous way as the adsorption energy [see Eq. (1)].

Using the C_6 coefficients obtained by the two different methods we added the dispersion correction to the energy of periodic structures in an *a posteori* fashion, i.e., the geom-

Author complimentary copy. Redistribution subject to AIP license or copyright, see http://jcp.aip.org/jcp/copyright.jsp

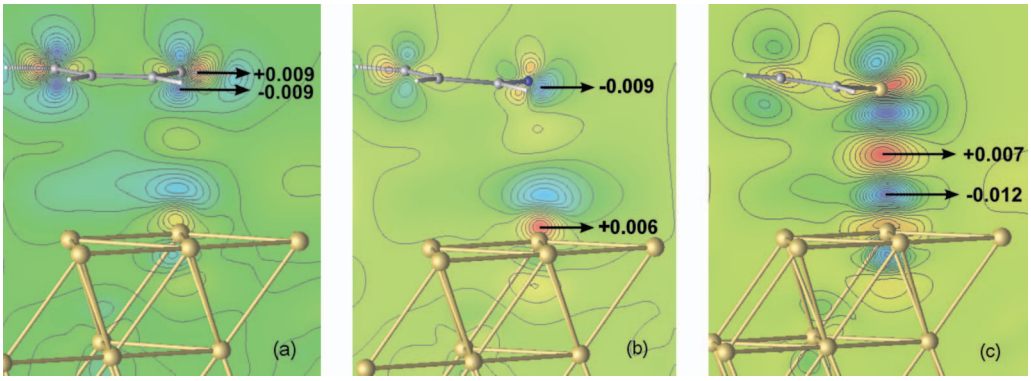

FIG. 1. Adsorption of (a) benzene, (b) pyridine, and (c) thiophene on Au(111). The contour plot illustrates the charge density difference upon adsorption of the molecules. The minimum and maximum charge density difference is given in $e/Å^3$. The spacing between the contour lines is 0.001 $e/Å^3$.

etries were not optimized in a self-consistent way. For the molecular configuration, we expect little changes of the optimum geometry including dispersion effects while the change of the energy minimum distance from the surface was determined by mapping out the corresponding potential curves. However, we are currently implementing the dispersion correction including forces into the periodic plane wave code so that a self-consistent structure optimization with dispersion corrections becomes possible.

We furthermore note that we have used a constant C_6 coefficient for all atoms of the same element, i.e., we have not taken into account any screening effects of the metal into the dispersion corrections, as recently discussed.[46] All five metal layers representing the (111) surface in the DFT-calculation were taken into account for the evaluation of the dispersion energy. Test calculations showed that the dispersion energy between, e.g., a thiophene and a Au(111) surface that are separated by 2.5 Å increases by less than 1.5 meV (2.5 meV) for the C_6 coefficient deduced from the QM:QM hybrid approach (Grimme approach) when an additional sixth Au layer is included. As far as lateral dimensions are concerned, the summation was done over all atoms within a sphere with a radius corresponding to nine surface unit cells. Increasing this radius to ten unit cells leads to changes of only 2.6×10^{-3} meV (4.3×10^{-3} meV).

III. RESULTS

A. Aromates in the gas phase

The optimized bond lengths and angles of benzene, pyridine and thiophene in the gas phase obtained from the DFT calculations are in good agreement with experimental values:[72,73] the maximal error in the bond lengths is 1.52% and in the bond angles it is 0.72%. The calculated dipole moments of thiophene (0.45 D) and pyridine (2.22 D) are close to experimental values as well.[74,75] In order to model the chemical nature of the adsorption processes correctly, the quality of the DFT description concerning the electronic properties of the isolated molecules is vitally important. Approximating the Kohn–Sham eigenvalues as ionization energies and comparing them to experimental ionization potentials obtained from photoelectron spectroscopy[76,77] shows that the eigenvalues underestimate the ionization energies by 3–4 eV which is a well-known problem of DFT calculations. Thus charge transfer from these molecules to, e.g., surfaces might be overestimated.

In the case of benzene and thiophene, the ordering of the molecular orbitals obtained by DFT calculations is consistent with experimental results. As far as pyridine is concerned, DFT calculations and photoelectron spectroscopy are at variance with each other with respect to the order of the two highest occupied molecular orbitals: PBE-DFT predicts the $11a_1(n)$ orbital to be the HOMO and the $1a_2(\pi)$ orbital to be 0.8 eV lower in energy, while results from photoelectron spectroscopy report the $1a_2(\pi)$ orbital to be 0.15 eV higher in energy than the $11a_1(n)$ orbital.[77] The hybrid functional B3LYP yields the same wrong ordering of the electronic states of pyridine close to the HOMO.[78] Although the energy difference between the two orbitals is relatively small, the underestimation of the $1a_2(\pi)$ orbital might slightly influence the orientation of the molecule on the surface.

B. Adsorption on Au(111)—pure DFT calculations without dispersion corrections

1. Adsorption geometry and energy

According to our PBE-DFT calculations, in the (3×3) overlayer structure thiophene adsorbs in a nearly flat manner with an adsorption energy of −0.09 eV. In this configuration, there is an angle between the molecular axis of the thiophene and the surface plane of 7.6° with the S-atom pointing toward the surface [see Fig. 1(c)]. The distance between the surface and the S-atom amounts to 3.4 Å. This flat-lying orientation is 40 meV more stable than the vertical one. At the most stable adsorption site the S-atom is located over a top position. Lateral translation leads to adsorption sites that are at most 40 meV higher in energy. Upon adsorption, the intermolecular bond lengths and angles of the thiophene molecule change less than 0.4% with respect to the corresponding values in the gas phase. The orientation of the molecule on the surface determined with DFT-PBE is consistent with experimental results at low coverage. However, experimental adsorption energies lie between −0.57 eV (Ref. 21) and −0.68 eV,[20] its absolute value is thus much higher than the calculated one.

At high coverage, experiments indicate that thiophene adsorbs in a $(\sqrt{3}\times\sqrt{3})R30°$ overlayer structure with

Author complimentary copy. Redistribution subject to AIP license or copyright, see http://jcp.aip.org/jcp/copyright.jsp

thiophene molecules standing upright.[12,21] In contrast to these findings no exothermic adsorption in such a densely packed monolayer was found by DFT-calculations (E_{ad}= +0.056 eV).

In agreement with previous theoretical studies,[28] pyridine was found to adsorb on Au(111) in a vertically oriented manner situated over a top position with the nitrogen atom bound to Au. In a (3×3) overlayer structure the vertical orientation has an adsorption energy of −0.28 eV and is about 0.22 eV more stable than the flat orientation. Among the flat-lying configurations of the adsorbed pyridine the most stable adsorption site is found for the N-atom again located over a top position. However, there is little corrugation as far as the location of the ring center is concerned: the energies vary by at most ΔE_{ad}=2 meV. As already shown by Bilić *et al.*,[28] varying the angle between the symmetry axis of pyridine and the Au surface from 0° to 20° only leads to minor changes in the adsorption energy. We have chosen an optimized adsorption geometry with an Au–N-distance of 3.5 Å and a tilting angle of 10° to model the adsorption of flat-lying pyridine. The changes in intermolecular bond lengths and angles relative to the pyridine in the gas phase are very small. In contrast to these calculational results at low coverages, the flat orientation was found to be the stable one in experiments.[17]

As far as the adsorption of benzene on Au(111) is concerned, we found that the most stable adsorption site is a threefold hollow position for the ring center of benzene [see Fig. 1(a)], again in agreement with calculations by Bilić *et al.*[27] However, our calculated adsorption energy of −0.03 eV is 0.05 eV smaller in its absolute value than the adsorption energy reported by Bilić *et al.* This discrepancy might be explained by the fact that we use more k-points to sample the irreducible Brillouin zone. The equilibrium distance from the surface is calculated to be 3.6 Å in contrast to 3.5 Å obtained by Bilić *et al.*[27] Changes in the molecular binding geometry of benzene upon adsorption are negligible (<0.05%). Our calculations confirm the experimentally determined flat adsorption geometry but underestimate the measured adsorption energy of −0.63 eV.[10]

The small adsorption energies, large distances from the surfaces and small changes in the bond lengths and angles compared to the molecules in the gas phase found in our calculations indicate that there is only a weak interaction taking place between the aromatic molecules and the metal surface. In order to get a deeper insight into the bonding situation, the next section will describe the electronic properties of the adsorption complex.

2. Electronic properties

In addition to the adsorption geometries, Fig. 1 shows contour maps of the adsorption induced electronic charge density difference for benzene, pyridine and thiophene on Au(111). Apparently, upon adsorption the electronic density is redistributed from the π- to the σ^*-orbitals of the aromate. In the case of benzene and pyridine the charge density is only slightly increased in the region between the adsorbate and the substrate. The charge redistribution is mainly localized at the molecule and at the surface. In contrast to benzene and pyridine, the major changes in electronic density due to the adsorption of thiophene take place in the region between the thiophene and the Au surface indicating that there is a contribution from covalent binding. However, in accordance with the small adsorption energy, the value of the charge density difference in this region is rather small, above all, compared to values for strongly adsorbed molecules such as methylthiolate with values of the charge density difference ranging from −0.20 to +0.08 e/Å^3 (Ref. 80).

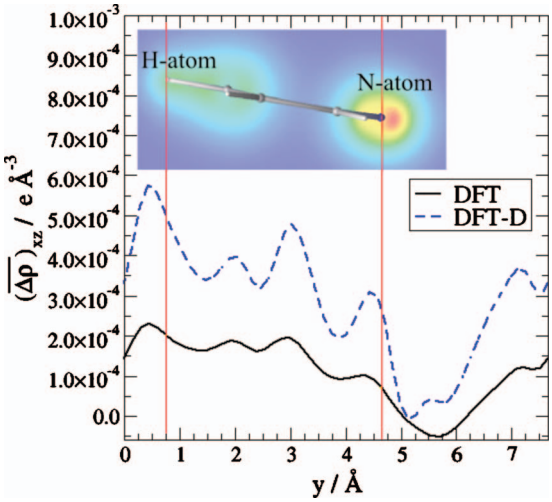

FIG. 2. Average charge density difference in the xz-plane taken at the surface for the equilibrium adsorption distance of pyridine on Au(111) derived from DFT (full line) and DFT-D (dashed line) calculations. The averaged region extends over the whole unit cell in x-direction and over 5 Å around the uppermost Au-layer in z-direction. The inset shows a 2D cut through the total electronic density of pyridine adsorbed on Au(111). The vertical lines assign the position of the N-atom and the opposing H-atom.

As pyridine has a rather strong dipole moment of 2.22 D (see Sec. III A), there might be also dipole-dipole forces contributing to the adsorption. The inset of Fig. 2 shows a two-dimensional (2D) cut through the total electronic density of pyridine adsorbed on Au(111). The cut is chosen to be perpendicular to the molecular plane and contains the symmetry axis of the molecule. Charge accumulates at the nitrogen atom revealing the dipole property of pyridine. Beneath, the average of the electronic charge density difference in the xz-plane in the region of the Au surface along the C_2 symmetry axis of pyridine is shown. The enhanced charge at the surface is not distributed evenly. In the region beneath the N-atom less charge density can be found, whereas in the region beneath the other end of the molecule charge accumulates. Hence, pyridine induces a dipole in the surface, but looking at numbers shows that this is also only a weak effect.

The tiny changes in the charge density redistribution go along with the small adsorption energies and large distances from the substrate. However, experimental measured adsorption energies are an order of magnitude larger. This discrepancy between calculations and experiments is most likely due to the dispersion effects missing in DFT-PBE. Section III C focuses on including dispersion effects in the DFT-calculations.

Author complimentary copy. Redistribution subject to AIP license or copyright, see http://jcp.aip.org/jcp/copyright.jsp

C. Corrections for dispersion effects

1. C_6 coefficients for metals

As mentioned above, we have determined the C_6 coefficients for Cu and Au both in the Grimme approach[37] and using a hybrid QM:QM method.[50,51] In the Grimme approach, the C_6 coefficients of elements are obtained, employing a simplified London formula with atomic ionization potentials and static dipole polarizabilities from DFT/PBE0 calculations. According to the original ansatz of Grimme,[37] the C_6 parameters of transition metal atoms can be obtained as a simple average of the C_6 parameters of the preceeding rare gas atom and the following group III element, but for comparison, we also calculated them explicitly.

In order to deduce C_6 coefficients for metal atoms via the hybrid approach, the adsorption of thiophene on Au and Cu in a flat-lying orientation was chosen as a model system. Single-point MP2 and DFT-PBE calculations of thiophene on small metal clusters were done. The structures of the metal clusters were taken from optimized metal substrate geometries obtained by periodic DFT-PBE calculations of the adsorption of the aromate on the extended (111) surface. The cluster geometry was kept fixed, and the spin was restricted to the singlet state to mimic the metallic nature of the extended substrates. For a given number of metal atoms, there are different possibilities to cut metal clusters out of the extended substrate. The shapes of the clusters taken into consideration for the calculation of the metallic C_6 coefficients were chosen carefully, since for some arbitrarily cut cluster structures convergence problems arose or calculations of the adsorption complex and the pure cluster led to different electronic configurations of the metal.

To verify the suitability of MP2 for interactions of aromates with metal clusters, further post-Hartree–Fock methods [MP3, MP4, CCSD, and CCSD(T)] were applied to the adsorption of thiophene on small Au clusters using LANL2DZ effective core potential for all atoms [see Fig. 3(a)]. As expected, MP2 overestimates the interactions between the metal cluster and the aromate. However, the error of MP2 in the interaction energy with respect to CCSD with perturbatively included triple excitations (CCSD(T)) is in the range of the error of other methods (MP3, MP4, and CCSD), in some cases even smaller.

As these calculations were only done with a double-zeta basis set for the atoms of thiophene, the influence of the basis set on the overestimation of dispersion effects in the MP2 calculations needs to be studied. Model calculations of the interaction between a Au-dimer and thiophene were carried out using CCSD and MP2 and various Gaussian type basis sets [6-31G, 6-311G, 6-311G(d,p), and 6-311G +(d,p)]. The calculations show that with an increasing basis set the difference between the interaction energy calculated with CCSD and the interaction energy calculated with MP2 increases. Going from a double to a triple valence basis set, the difference in the interaction energies increases from 6.9 to 9.9 meV.

Adding polarization functions has a huge impact and the difference between the CCSD and the MP2 calculations is further increased to 33.5 meV. By adding diffuse functions to the basis the difference between CCSD and MP2 is hardly influenced (increase of less than 2%). In total, using the 6-311G+(d,p) basis set, MP2 calculations overestimate the interaction energy of this system by 34.2 meV corresponding to 28% with respect to CCSD calculations. Since CCSD rather underestimates the interaction of thiophene with such small Au clusters compared to CCSD(T), the error of 28% of MP2 might be seen as an upper limit.

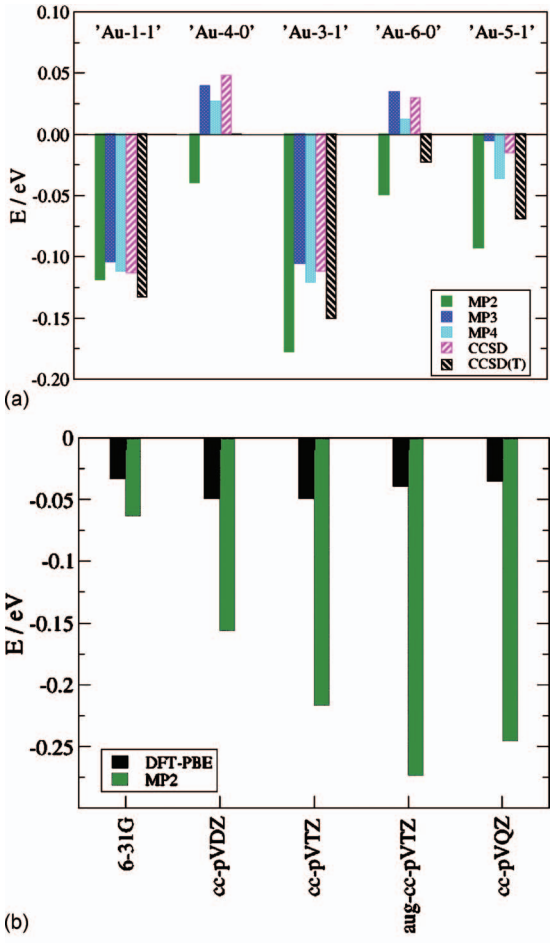

FIG. 3. Interaction energy between thiophene and Au clusters. In (a), different post-Hartree–Fock methods were applied to the interaction of thiophene with various Au clusters. Here Au-x-y denotes a Au cluster where x atoms were taken from the uppermost layer and y atoms were taken from the second layer of the slab. The LANL2DZ effective core potential was used for all atoms. In (b), different basis sets for the atoms of thiophene were used for MP2 and DFT-PBE calculations of the interaction energy between thiophene and an Au 6-0 cluster. For the Au atoms the LANL2DZ effective core potential was used.

In summary, these tests show that MP2 seems to be suitable for the description of the adsorption of thiophene on small Au clusters, in spite of the fact that it is in general not well-suited to describe metals. One has to keep in mind that finite metal clusters still have discrete energy levels and a HOMO-LUMO gap so that a perturbative approach is in principle possible. However, it should furthermore be borne in mind, that MP2 slightly overestimates dispersion effects.

Since we are interested in the reliable difference between MP2 and PBE calculations, the influence of the basis set on the interaction energies of these methods needs to be studied as well. A 2D Au cluster containing six Au atoms was em-

Author complimentary copy. Redistribution subject to AIP license or copyright, see http://jcp.aip.org/jcp/copyright.jsp

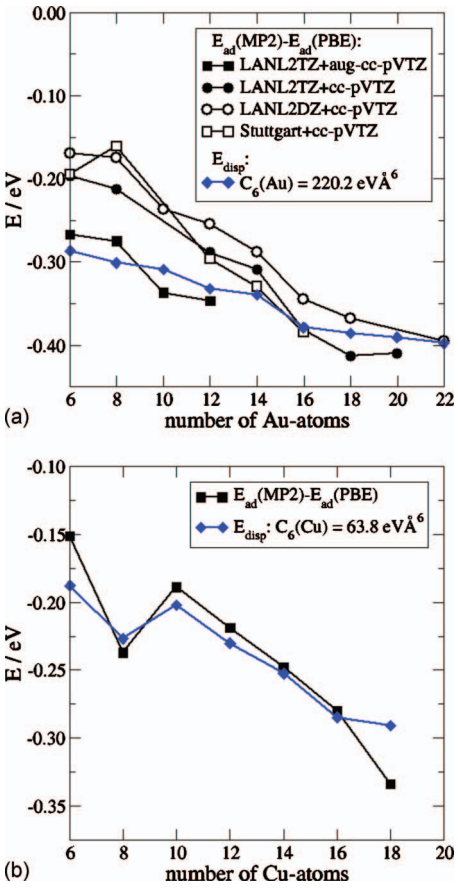

FIG. 4. Least-squares fitting of E_{disp} (blue curve) to $E_{\mathrm{ad}}(MP2)-E_{\mathrm{ad}}(PBE)$ (black curves) for thiophene adsorbing on (a) Au clusters and (b) Cu clusters. In (a) various effective core potentials for Au atoms and different basis sets for the atoms of the thiophene molecule are shown, while in (b) the LANL2TZ effective core potential was used for Cu atoms and the augmented correlation consistent basis set of Dunning (aug-cc-pVTZ) was used for the thiophene atoms. Connecting lines are just a guide to the eyes.

ployed for model calculations of the interaction between Au and thiophene. Figure 3(b) shows that increasing the basis has hardly any influence on the PBE interaction energy. In contrast, the MP2 interaction energy increases drastically by going from double to triple valence basis functions and by adding polarization functions. Besides, Fig. 3(b) shows that the augmentation of Dunning's correlation consistent basis set with diffuse functions has a strong influence on the interaction energy difference between MP2 and PBE and is therefore inevitable, at least for adsorption complexes with small metal clusters.

In Fig. 4, the difference between the adsorption energy of a MP2 calculation and of a DFT-PBE calculation is plotted against the number of metal atoms in the cluster. A least-squares fitting of the dispersion expression to this difference leads to C_6 coefficients of 220.2 eV Å^6 for Au and 63.8 eV Å^6 for Cu. The calculations for different basis sets and different effective core potentials in Fig. 4(a) show that the adsorption energy difference depends to a larger extent on the basis set of the thiophene atoms than on the effective core potential and the basis set used for the Au atoms.

In Table II, the obtained values for the C_6 coefficients of metal atoms are compared to the values calculated via the Grimme approach. The C_6 parameters obtained as average of the C_6 parameters of the preceeding rare gas and the following group III elements differ by 56% (Cu) and 10% (Au) from the explicitly calculated C_6 parameters. An even stronger deviation of 75% (Cu) and 61% (Au) can be found for the C_6 coefficients deduced from the QM:QM hybrid approach. However, there is a good agreement between the C_6 parameter of Au deduced from the QM:QM hybrid approach and a recently published Au-C_6 value of 179.2 eV Å^6 calculated via a fitting to C_3 parameters appearing in the z^{-3} interaction between a molecule and a surface.[48] Interestingly enough, the C_6 parameters deduced from atomic properties compare rather well with C_6 parameters derived from a Lennard-Jones 6-12 potential ansatz to reproduce bulk metal properties.[81,82] In this approach, the Lennard-Jones parameters reflect the total metal-metal interaction and not only the van der Waals interaction. This might be a first hint that the C_6 parameters for free metal atoms deduced from the Grimme approach are probably too large to be an adequate model for the C_6 parameters describing dispersion effects of atoms in metal surfaces. This will be confirmed in the next section where we will apply the DFT-D correction to the adsorption energies of the aromates using the different sets of calculated C_6 coefficients.

2. DFT-D results

Figure 5 shows the adsorption energy for thiophene on Au(111) and Cu(111) as a function of the metal-sulfur distance. DFT-D calculations were carried out using C_6 values for metals deduced from both the Grimme ansatz and the QM:QM hybrid approach. Due to dispersion effects the equilibrium distance of the interaction between thiophene and the Au surface is shifted from 3.4 to 2.88 Å for C_6(Au) =220 eV Å^6 and to 2.75 Å for C_6(Au)=615 eV Å^6. With respect to the adsorption on Cu(111) this distance decreases from 3 to 2.4 Å for both C_6 coefficients. Hence, the difference in the C_6 coefficients calculated via different methods does not influence the equilibrium distance markedly. However, it has a large impact on the adsorption energies. The DFT value of the adsorption energy for thiophene on Au(111) is corrected from −0.09 to −0.73 eV (−1.24 eV) by adding dispersion effects with C_6(Au)=220 eV Å^6 (C_6(Au)=615 eV Å^6). A similar effect can be seen for the adsorption of thiophene on Cu(111): the adsorption energy decreases from −0.07 to −0.61 eV for C_6(Cu)=64 eV Å^6 and to −0.81 eV for C_6(Cu)=112 eV Å^6. Comparisons to experiments show, that adding dispersion effects in a semiempirical fashion with the metal C_6 coefficients deduced from the QM:QM hybrid approach leads to adsorption energies that are in the range of the experimental measured values [Au: −0.57 eV (Ref. 21) and −0.68 eV (Ref. 20); Cu: −0.59 eV (Ref. 18)]. For the adsorption of thiophene on Cu(111) not only the adsorption energy, but also the distance between the sulfur atom and the Cu surface was measured. Normal incidence x-ray standing wavefield absorption revealed a Cu–S separation of 2.62 ± 0.03 Å.[18] By near edge X-ray absorption fine structure (NEXAFS) experiments at the S K-edge, the distance was found to be 2.50 ± 0.02 Å.[83] Again there is a good agreement between the calculated and the measured value.

Author complimentary copy. Redistribution subject to AIP license or copyright, see http://jcp.aip.org/jcp/copyright.jsp

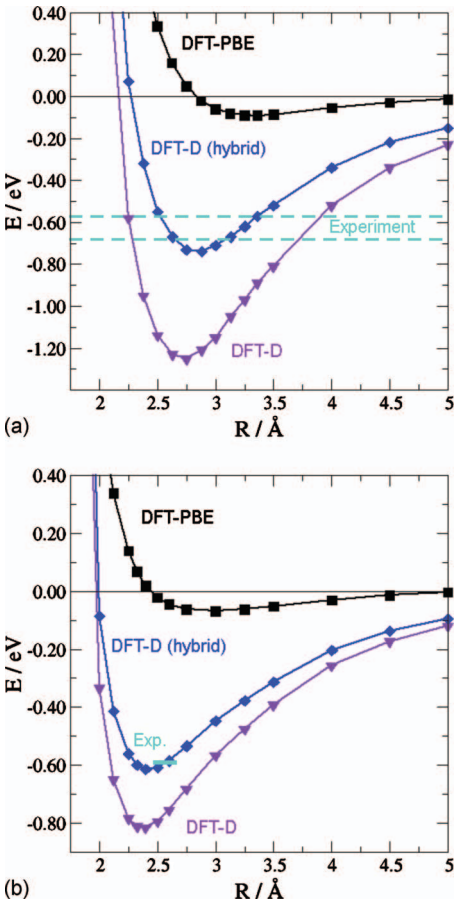

FIG. 5. Adsorption energies of thiophene on (a) Au(111) and (b) Cu(111) calculated with different methods [DFT-PBE (black boxes), DFT-D: Grimme (indigo triangles), and DFT-D: hybrid (blue diamonds)] and compared to the range of experimental values (dashed lines, see text). Connecting lines are just a guide to the eyes.

Potential energy curves for other aromates on these surfaces are very similar. In Table I, adsorption energies are summarized. For all aromates and both substrates the adsorption energies calculated with the hybrid DFT-D approach compare well with experimental values from thermal desorption experiments as far as they are available.

Very recently, it was proposed to calculate the C_6 coefficients employing a new concept of fractional coordination numbers to interpolate between *ab initio* derived dispersion coefficients of atoms in different chemical environments.[38] Using this approach, we obtain C_6 values for Cu and Au of 104.6 and 189.6 eV Å^6, respectively, in metallic environments. In particular the value for Au is rather close to our value obtained within the hybrid approach, the difference only amounts to 14%. For Cu, the difference is 63%, however, this leads to changes in the total adsorption energy of less than 0.2 eV, as Fig. 5(b) illustrates, where the DFT-D results were obtained with a C_6 coefficient of 112 eV Å^6.

As dispersive interactions bring the aromates closer to the surface, there might also be changes in the electronic properties of the adsorption complex. Note that the inclusion of the dispersion corrections does not directly change the electronic structure but indirectly through the modified minimum energy adsorption geometry. Figure 6 shows a 2D cut through the charge density difference of the adsorption of (a) benzene, (b) pyridine, and (c) thiophene on Au(111) at their equilibrium distances determined with DFT-D. Qualitatively, almost no differences can be seen when this 2D cut is compared to the contour plot of the corresponding charge density difference at the equilibrium distance obtained by the pure DFT calculation presented in Fig. 1. However, the values of the maximal and minimal charge density difference clearly reveal that much more charge is shifted from the region close to the Au surface and the molecule to the region in between the two reactants, when the molecule comes closer to the surface. Hence, the contribution of covalent binding is increased for the adsorption of all three aromates on Au(111), if dispersion effects are included. For the adsorption of pyridine on Au we have already seen in the pure DFT calculation, that there are also dipole-dipole interactions slightly contributing to the binding situation (see Sec. III B 2). In Fig. 2, the influence of the smaller adsorption distance derived by the DFT-D calculation on the dipole moment induced in the surface is plotted: compared to the adsorption distance derived by pure DFT calculations, the gradient between the charge density differences beneath the H- and the N-atom is steeper and therefore a larger dipole moment is induced in the surface and the dipole-dipole interactions are enhanced.

So far we have seen that adding dispersive interactions leads to significant changes compared to pure DFT calculations. Furthermore we want to know whether this DFT-D approach is also helpful, if DFT fails completely in describing the qualitative trends that are observed in experiment. As shown in Sec. III B 1 pure DFT calculations could not reproduce the stability of experimentally observed densely packed monolayers of thiophene on Au(111). By adding dispersion corrections to the adsorption of thiophene in a ($\sqrt{3}$

TABLE I. Adsorption energies (in eV) of aromatic molecules on Cu(111) and Au(111) in a flatly oriented adsorption geometry calculated with different methods and compared to experimental values.

	E_{ad}^{DFT}	$E_{ad}^{DFT\text{-}D}$		$E_{ad}^{Expt.}$	
		Hybrid	Grimme		Ref.
Au/benzene	−0.03	−0.76	−1.35	−0.63	10
Au/pyridine	−0.06	−0.71	−1.26	Not available	
Au/thiophene	−0.09	−0.73	−1.24	−0.57; −0.68	20 and 21
Cu/benzene	−0.02	−0.61	−0.86	−0.59	8
Cu/pyridine	−0.06	−0.59	−0.82	−0.52; −0.56	22 and 79
Cu/thiophene	−0.07	−0.61	−0.81	−0.59	18

Author complimentary copy. Redistribution subject to AIP license or copyright, see http://jcp.aip.org/jcp/copyright.jsp

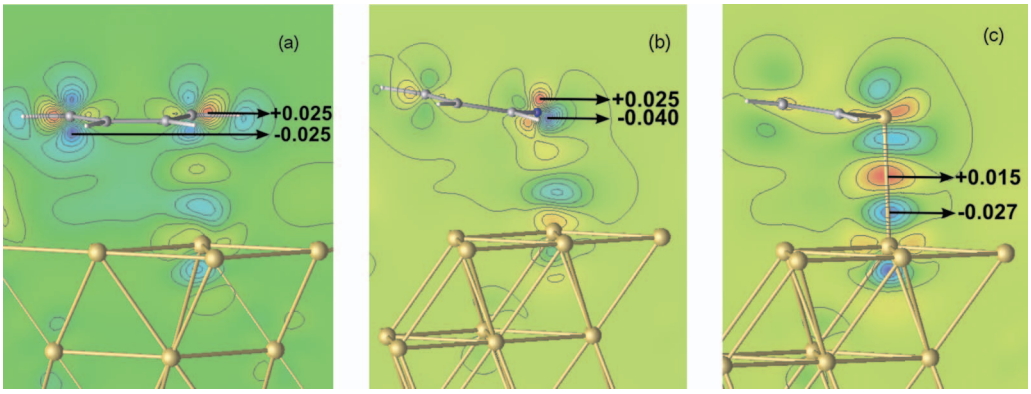

FIG. 6. Contour plot of the charge density difference of the adsorption of (a) benzene, (b) pyridine, and (c) thiophene on Au(111) at their corresponding equilibrium distance determined with DFT-D. The minimum and maximum charge density difference is given in $e/Å^3$. Step size of contours 0.005 $e/Å^3$.

$\times\sqrt{3})R30°$ unit cell a stable adsorption complex with an adsorption energy of −0.34 eV is obtained. This value is close to the experimentally determined value [−0.48 eV (Ref. 21)]. In such densely packed monolayers the dispersive forces between neighboring molecules become quite important. For example, in the $(\sqrt{3}\times\sqrt{3})R30°$ overlayer structure they represent 36% of the total dispersive energy. For a smaller coverage of one molecule per (3×3) surface unit cell, dispersive interactions between adjacent molecules are rather negligible (<0.8%). As the C_6 coefficients were determined for flat-lying physisorbed molecules it is questionable whether this approach is also applicable for vertical standing aromates. Therefore the adsorption of thiophene in a $(\sqrt{3}\times\sqrt{3})R30°$ overlayer structure was also calculated by modeling the Au substrate by a Au_6 cluster. MP2 calculation, as well as DFT and DFT-D, was employed. Figure 7 shows the comparison of the three methods. DFT leads only to a weak stable state (E_{ad}=−0.02 eV) at a distance of 3.75 Å, whereas MP2 indicates a stronger adsorption (E_{ad}=−0.18 eV) at a separation of 3.25 Å. By adding dispersion corrections to DFT the resulting potential energy curve is in good agreement with the potential energy curve obtained by MP2 calculations. This indicates that our parameters derived for flat-lying adsorbed aromates are also transferable to other molecular orientations so that it can also be applied to the DFT description of self-assembled monolayers.[84,85]

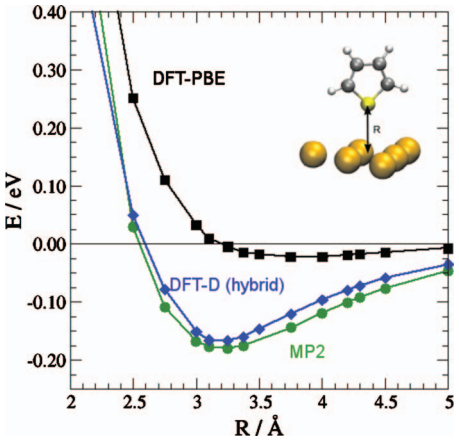

FIG. 7. Interaction energy between thiophene and an Au-6-0 cluster calculated with different methods [DFT-PBE (black boxes), DFT-D: hybrid (blue diamonds), and MP2 (green circles)] and the effective core potential LANL2TZ for Au and the aug-cc-pVTZ basis set for S, C, and H-atoms.

A further example where DFT fails to describe the experimental observations is the adsorption of pyridine on Au(111) at low coverage. Experiments report flat-lying molecules on the surfaces, whereas DFT calculation finds the vertically adsorbed pyridine to be more stable. Adding dispersion effects leads to adsorption energies of −0.71 eV for the flat configuration and −0.79 eV for the vertical configuration. Still, the vertical configuration is more stable, but the difference in the adsorption energies decreases to only 0.08 eV. In Sec. III A, we pointed out that DFT fails in describing the experimentally observed ordering of the highest occupied molecular orbitals as well as their relative energies. The influence of the electron lone pair at the N-atom is overestimated by DFT which might explain why the vertical configuration is erroneously favored.

IV. CONCLUSIONS

The adsorption of the simple aromatic molecules benzene, thiophene and pyridine on Au(111) and Cu(111) has been studied using periodic DFT calculations. A pure DFT-GGA approach leads to adsorption energies that are significantly underestimated compared to experimental results. Adding dispersion corrections within a DFT-D approach based on atomic properties causes an overbinding to the metal substrates. Good agreement between theory and experiment is achieved, for the adsorption of both isolated molecules as well as denser overlayer structures, when the dispersion corrections are based on a QM:QM hybrid approach. Thus this computationally inexpensive approach offers an

TABLE II. C_6 coefficients for metal-atoms calculated with different methods (in eV $Å^6$).

	Cu	Au
Hybrid approach[a]	64	220
Grimme approach[b]	256	558
Grimme approach, average[b,c]	112	615

[a]References 50 and 51.
[b]UDFT-PBE0/QZVP computations (see Ref. 37).
[c]Average of preceeding group VIII and following group III element (see Ref. 37).

Author complimentary copy. Redistribution subject to AIP license or copyright, see http://jcp.aip.org/jcp/copyright.jsp

attractive alternative to very costly DFT calculations employing nonlocal van der Waals density functionals.

ACKNOWLEDGMENTS

We thank Christian Mosch for technical support. Furthermore, we thank Stefan Grimme for helpful discussions concerning the DFT-D approach, for sending us a manuscript prior to publication and for technical support in the evaluation of C_6 parameters.

[1] J. R. Heath and M. A. Ratner, Phys. Today **56**(5), 43 (2003).
[2] U. Mitschke and P. Bäuerle, J. Mater. Chem. **10**, 1471 (2000).
[3] A. Groß, J. Comput. Theor. Nanosci. **5**, 894 (2008).
[4] C.-Q. Ma, E. Mena-Osteritz, T. Debaerdemaeker, M. M. Wienk, R. A. J. Janssen, and P. Bäuerle, Angew. Chem., Int. Ed. **46**, 1679 (2007).
[5] C. Meier, K. Landfester, D. Künzel, T. Markert, A. Groß, and U. Ziener, Angew. Chem., Int. Ed. **47**, 3821 (2008).
[6] D. Künzel, T. Markert, A. Groß, and D. M. Benoit, Phys. Chem. Chem. Phys. **11**, 8867 (2009).
[7] C. Meier, M. Roos, D. Künzel, A. Breitruck, H. E. Hoster, K. Landfester, A. Gross, R. J. Behm, and U. Ziener, J. Phys. Chem. C **114**, 1268 (2010).
[8] M. Xi, M. X. Yang, S. Jo, and B. E. Bent, J. Chem. Phys. **101**, 9122 (1994).
[9] X.-L. Zhou, M. E. Castro, and J. M. White, Surf. Sci. **238**, 215 (1990).
[10] D. Syomin, J. Kim, B. E. Koel, and G. B. Ellison, J. Phys. Chem. B **105**, 8387 (2001).
[11] R. Dudde, K.-H. Frank, and E.-E. Koch, Surf. Sci. **225**, 267 (1990).
[12] G.-J. Su, H.-M. Zhang, L.-J. Wan, and C.-L. Bai, Surf. Sci. **531**, L363 (2003).
[13] T. Matsuura, M. Nakajima, and Y. Shimoyama, Jpn. J. Appl. Phys., Part 1 **40**, 6945 (2001).
[14] T. Matsuura and Y. Shimoyama, Eur. Phys. J. E **7**, 233 (2002).
[15] J. Lipkowski, L. Stolberg, D.-F. Yang, B. Pettinger, S. Mirwald, F. Henglein, and D. M. Kolb, Electrochim. Acta **39**, 1045 (1994).
[16] L. Stolberg, S. Morin, J. Lipkowski, and D. E. Irish, J. Electroanal. Chem. **307**, 241 (1991).
[17] W.-B. Cai, L.-J. Wan, H. Noda, Y. Hibino, K. Ataka, and M. Osawa, Langmuir **14**, 6992 (1998).
[18] P. K. Milligan, B. Murphy, D. Lennon, B. C. C. Cowie, and M. Kadodwala, J. Phys. Chem. B **105**, 140 (2001).
[19] P. Väterlein, M. Schmelzer, J. Taborski, T. Krause, F. Viczian, M. Bäßler, R. Fink, E. Umbach, and W. Wurth, Surf. Sci. **452**, 20 (2000).
[20] G. Liu, J. A. Rodriguez, J. Dvorak, J. Hrbek, and T. Jirsek, Surf. Sci. **505**, 295 (2002).
[21] A. Nambu, H. Kondoh, I. Nakai, K. Amemiya, and T. Ohta, Surf. Sci. **530**, 101 (2003).
[22] Q. Zhong, C. Gahl, and M. Wolf, Surf. Sci. **496**, 21 (2002).
[23] J. E. Demuth, K. Christmann, and P. N. Sanda, Chem. Phys. Lett. **76**, 201 (1980).
[24] M. H. Dishner, J. C. Hemminger, and F. J. Feher, Langmuir **12**, 6176 (1996).
[25] J. Noh, E. Ito, K. Nakajima, J. Kim, H. Lee, and M. Hara, J. Phys. Chem. B **106**, 7139 (2002).
[26] G. Andreasen, M. E. Vela, R. C. Salvarezza, and A. J. Arvia, Langmuir **13**, 6814 (1997).
[27] A. Bilić, J. R. Reimers, N. S. Hush, R. C. Hoft, and M. J. Ford, J. Chem. Theory Comput. **2**, 1093 (2006).
[28] A. Bilić, J. R. Reimers, and N. S. Hush, J. Phys. Chem. B **106**, 6740 (2002).
[29] S. Higai, J. Nara, and T. Ohno, Surf. Sci. **600**, 685 (2006).
[30] O. A. von Lilienfeld, I. Tavernelli, U. Rothlisberger, and D. Sebastiani, Phys. Rev. Lett. **93**, 153004 (2004).
[31] Y. Zhao and D. G. Truhlar, J. Chem. Phys. **125**, 194101 (2006).
[32] M. Dion, H. Rydberg, E. Schröder, D. C. Langreth, and B. I. Lundqvist, Phys. Rev. Lett. **92**, 246401 (2004).
[33] P. Sony, P. Puschnig, D. Nabok, and C. Ambrosch-Draxl, Phys. Rev. Lett. **99**, 176401 (2007).
[34] N. Atodiresei, V. Caciuc, P. Lazić, and S. Blügel, Phys. Rev. Lett. **102**, 136809 (2009).
[35] Q. Wu and W. Yang, J. Chem. Phys. **116**, 515 (2002).
[36] S. Grimme, J. Comput. Chem. **25**, 1463 (2004).
[37] S. Grimme, J. Comput. Chem. **27**, 1787 (2006).
[38] S. Grimme, J. Antony, S. Ehrlich, and H. Krieg, J. Chem. Phys. **132**, 154104 (2010).
[39] E. R. Johnson and A. D. Becke, J. Chem. Phys. **123**, 024101 (2005).
[40] P. Jurečka, J. Černý, P. Hobza, and D. R. Salahub, J. Comput. Chem. **28**, 555 (2007).
[41] F. Ortmann, F. Bechstedt, and W. G. Schmidt, Phys. Rev. B **73**, 205101 (2006).
[42] A. Tkatchenko and M. Scheffler, Phys. Rev. Lett. **102**, 073005 (2009).
[43] N. Marom, A. Tkatchenko, M. Scheffler, and L. Kronik, J. Chem. Theory Comput. **6**, 81 (2010).
[44] F. Ortmann, W. G. Schmidt, and F. Bechstedt, Phys. Rev. Lett. **95**, 186101 (2005).
[45] N. Atodiresei, V. Caciuc, J.-H. Franke, and S. Blügel, Phys. Rev. B **78**, 045411 (2008).
[46] E. R. McNellis, J. Meier, and K. Reuter, Phys. Rev. B **80**, 205414 (2009).
[47] G. Mercurio, E. R. McNellis, I. Martin, S. Hagen, F. Leyssner, S. Soubatch, J. Meyer, M. Wolf, P. Tegeder, F. S. Tautz, and K. Reuter, Phys. Rev. Lett. **104**, 036102 (2010).
[48] M.-T. Nguyen, C. A. Pignedoli, M. Treier, R. Fasel, and D. Passerone, Phys. Chem. Chem. Phys. **12**, 992 (2010).
[49] C. Tuma and J. Sauer, Chem. Phys. Lett. **387**, 388 (2004).
[50] C. Tuma and J. Sauer, Phys. Chem. Chem. Phys. **8**, 3955 (2006).
[51] Q.-M. Hu, K. Reuter, and M. Scheffler, Phys. Rev. Lett. **98**, 176103 (2007).
[52] G. Kresse and J. Furthmüller, Phys. Rev. B **54**, 11169 (1996).
[53] G. Kresse and J. Furthmüller, Comput. Mater. Sci. **6**, 15 (1996).
[54] J. P. Perdew, K. Burke, and M. Ernzerhof, Phys. Rev. Lett. **77**, 3865 (1996).
[55] P. E. Blöchl, Phys. Rev. B **50**, 17953 (1994).
[56] G. Kresse and D. Joubert, Phys. Rev. B **59**, 1758 (1999).
[57] M. J. Frisch, G. W. Trucks, H. B. Schlegel, *et al.*, GAUSSIAN 03, Revision D.01, Gaussian, Inc., Wallingford, CT, 2004.
[58] P. J. Hay and W. R. Wadt, J. Chem. Phys. **82**, 270 (1985).
[59] P. J. Hay and W. R. Wadt, J. Chem. Phys. **82**, 299 (1985).
[60] W. R. Wadt and P. J. Hay, J. Chem. Phys. **82**, 284 (1985).
[61] D. Andrae, U. Haeussermann, M. Dolg, H. Stoll, and H. Preuss, Theor. Chem. Acc. **77**, 123 (1990).
[62] T. H. Dunning, Jr., J. Chem. Phys. **90**, 1007 (1989).
[63] R. A. Kendall, T. H. Dunning, Jr., and R. J. Harrison, J. Chem. Phys. **96**, 6796 (1992).
[64] R. Ditchfield, W. J. Hehre, and J. A. Pople, J. Chem. Phys. **54**, 724 (1971).
[65] W. J. Hehre, R. Ditchfield, and J. A. Pople, J. Chem. Phys. **56**, 2257 (1972).
[66] P. C. Hariharan and J. A. Pople, Theor. Chem. Acc. **28**, 213 (1973).
[67] P. C. Hariharan and J. A. Pople, Mol. Phys. **27**, 209 (1974).
[68] M. M. Francl, W. J. Pietro, W. J. Hehre, J. S. Binkley, D. J. DeFrees, J. A. Pople, and M. S. Gordon, J. Chem. Phys. **77**, 3654 (1982).
[69] A. D. McLean and G. S. Chandler, J. Chem. Phys. **72**, 5639 (1980).
[70] R. Krishnan, J. S. Binkley, R. Seeger, and J. A. Pople, J. Chem. Phys. **72**, 650 (1980).
[71] S. F. Boys and F. Bernardi, Mol. Phys. **19**, 553 (1970).
[72] W. R. Harshbarger and S. H. Bauer, Acta Crystallogr., Sect. B: Struct. Crystallogr. Cryst. Chem. **26**, 1010 (1970).
[73] D. Mootz and H.-G. Wussuw, J. Chem. Soc. **75**, 1517 (1981).
[74] M. E. Colnay, A. Vasseur, and M. Guerin, J. Chem. Res. Miniprint **9**, 2050 (1983).
[75] Z. Pawełka, B. Palasek, and A. Puszko, J. Phys. Org. Chem. **10**, 835 (1997).
[76] P. J. Derrick, L. Asbrink, O. Edqvist, B.-O. Jonsson, and E. Lindholm, Int. J. Mass Spectrom. Ion Phys. **6**, 191 (1971).
[77] M. S. Moghaddam, A. D. O. Bawagan, K. H. Tan, and W. von Niessen, Chem. Phys. **207**, 19 (1996).
[78] S. Tixier, W. A. Shapley, Y. Zheng, D. P. Chong, C. E. Brion, Z. Shi, and S. Wolfe, Chem. Phys. **270**, 263 (2001).
[79] P. R. Davies and N. Shukla, Surf. Sci. **322**, 8 (1995).

Author complimentary copy. Redistribution subject to AIP license or copyright, see http://jcp.aip.org/jcp/copyright.jsp

[80] L. M. Molina and B. Hammer, Chem. Phys. Lett. **360**, 264 (2002).
[81] P. M. Agrawal, B. M. Rice, and D. L. Thompson, Surf. Sci. **515**, 21 (2002).
[82] T. Halicioğlu and G. M. Pound, Phys. Status Solidi A **30**, 619 (1975).
[83] A. Imanishi, T. Yokoyama, Y. Kitajima, and T. Ohta, Bull. Chem. Soc. Jpn. **71**, 831 (1998).
[84] J. Kučera and A. Groß, Langmuir **24**, 13985 (2008).
[85] J. Kučera and A. Groß, Phys. Chem. Chem. Phys. **12**, 4423 (2010).

Author complimentary copy. Redistribution subject to AIP license or copyright, see http://jcp.aip.org/jcp/copyright.jsp